HHS Public Access

Author manuscript

Biochem Pharmacol. Author manuscript; available in PMC 2019 October 01.

Published in final edited form as:

Biochem Pharmacol. 2018 October ; 156: 32–42. doi:10.1016/j.bcp.2018.08.003.

Quantitative characterization of UDP-glucuronosyltransferase 2B17 in human liver and intestine and its role in testosterone first-pass metabolism

Haeyoung Zhang[a], **Abdul Basit**[a], **Diana Busch**[b], **King Yabut**[a], **Deepak Kumar Bhatt**[a], **Marek Drozdzik**[c], **Marek Ostrowski**[d], **Albert Li**[e], **Carol Collins**[a], **Stefan Oswald**[b], and **Bhagwat Prasad**[a]

[a]Department of Pharmaceutics, University of Washington, Seattle, WA, USA [b]Department of Clinical Pharmacology, University of Greifswald, Greifswald, Germany [c]Department of Experimental and Clinical Pharmacology, Pomeranian Medical University, Szczecin, Poland [d]Department of General and Transplantation Surgery, Pomeranian Medical University, Szczecin, Poland [e]In Vitro ADMET Laboratories (IVAL), Columbia, MD, USA

Abstract

Protein abundance and activity of UGT2B17, a highly variable drug- and androgen-metabolizing enzyme, was quantified in microsomes, S9, and primary cells isolated from human liver and intestine by a validated LC-MS/MS methods. UGT2B17 protein abundance showed >160-fold variation (mean ± SD, 1.7 ± 2.7 pmol/mg microsomal protein) in adult human liver microsomes (n=26) and significant correlation (r^2= 0.77, p<0.001) with TG formation. Primary role of UGT2B17 in TG formation compared to UGT2B15 was confirmed by performing the activity assay in UGT2B17 gene deletion samples and with a selective UGT2B17 inhibitor, imatinib. Human intestinal microsomes isolated from small intestine (n=6) showed on average significantly higher protein abundance (7.4 ± 6.6 pmol/mg microsomal protein, p=0.016) compared to liver microsomes, with an increasing trend towards distal segments of gastrointestinal (GI) tract. Commercially available pooled microsomes and S9 fractions confirmed greater abundance and activity of UGT2B17 in intestinal fractions compared to liver fractions. To further investigate the quantitative role of UGT2B17 in testosterone metabolism in whole cell system, a targeted metabolomics study was performed in hepatocytes (n=5), and enterocytes (n=16). TG was the second most abundant metabolite after androstenedione in both cell systems. Reasonable correlation between UGT2B17 abundance and activity were observed enterocytes (r^2=0.69, p=0.003), but not in hepatocytes. These observational and mechanistic data will be useful in

Corresponding author: Bhagwat Prasad, Ph.D.; Department of Pharmaceutics, University of Washington, 1959 NE Pacific Street, Seattle, WA 98195, Phone: (206) 221-2295, Fax: (206) 543-3204; bhagwat@uw.edu.

Conflict of interest

The authors declare no conflicts of interest.

developing a physiologically-based pharmacokinetic (PBPK) model for predicting highly-variable first-pass metabolism of testosterone and other UGT2B17 substrates.

Graphical Abstract

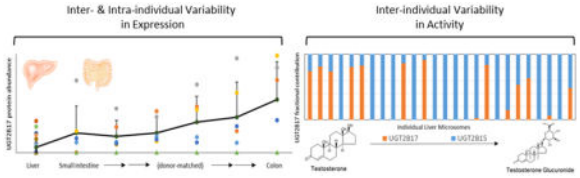

Keywords

UGT2B17; glucuronidation; testosterone; first-pass metabolism; metabolomics; inter-individual variability

1. Introduction

UGT2B17 is highly variable in its abundance and is one of the most commonly deleted genes in humans, with a higher deletion frequency seen in Asians [1]. Recently, we have shown that other than copy number variation (CNV), multiple factors contribute to its variability, including sex, age, and single nucleotide polymorphisms [2]. In addition to variable pharmacokinetics (PK) and efficacy or toxicity of drugs (e.g. vorinostat) [3], drug metabolites (e.g., 17-dihydroexemestane) [4], and tobacco carcinogen (NNAL) [5], UGT2B17 variability has been associated with various testosterone-related clinical outcomes [6–13]. For example, studies show that UGT2B17 deletion individuals have 15% higher serum testosterone levels [6] and up to 90% lower urinary excretion of conjugated plus unconjugated testosterone [7]. UGT2B17 gene deletion is well recognized as major confounder for anti-doping tests in athletes that can produce false positive and negative results [8], and is also associated with lower body mass index in males in a sex-specific manner [9,10]. Similarly, although controversial [11], a genome-wide CNV study found a strong link between UGT2B17 deletion and lower osteoporosis risk [6]. In addition, recent meta-analyses show increased prostate cancer risk with UGT2B17 gene deletion, amidst conflicting results [12,13].

Testosterone levels decline steadily after age thirty, reaching hypogonadal levels in approximately 20% to 50% of men in their 60s and 80s, respectively [14]. Symptomatic hypogonadism is treated with exogenous administration of testosterone, which leads to improvements in fatigue, muscle strength, body mass index, and mood [15]. In 2011 alone, 3.8% of men in their 60s were on testosterone replacement therapy (TRT). TRT is available in the United States (US) in various forms, i.e., transdermal, intramuscular, nasal, buccal, and subdermal. Oral formulations approved in the US are prodrug formulations alkylated testosterone which accompanies increased risks of hepatotoxicity such as cholestatic jaundice, therefore limiting its use [16,17]. , Esterified prodrug testosterone undecanoate has been used in Canada [18] and in Europe since 1970s without risk of liver damage [19]. However, it requires co-consumption with a fatty meal due to its lymphatic absorption and

has potential concerns regarding elevated dihydrotestosterone (DHT) levels [20,21]. Despite advantages of greater patient adherence and ease of use, oral testosterone formulations have been generally unsuccessful due to significant first-pass metabolism [15,20,22].

To develop a viable oral testosterone formulation, it is important to characterize factors responsible for its low and variable absolute bioavailability (3.6 ± 2.5 %) [23]. Intravenous testosterone is rapidly eliminated with a half-life ranging from 10 to 100 minutes with majority of testosterone excreted as glucuronide conjugates (up to 80%), suggesting extensive involvement of hepatic UGTs [24]. UGT2B17 and UGT2B15 are the major and minor isoforms responsible for TG formation, respectively [25], both of which are expressed in the liver. Moreover, UGT2B17 is also expressed in the intestine [26]. While these data indicate importance of UGT2B17 in testosterone first-pass metabolism, the quantitative role of intestinal and hepatic UGT2B17 has not been elucidated. Therefore, we first examined the abundance and testosterone glucuronidation activity of UGT2B17 and UGT2B15 in adult human liver and intestinal subcellular fractions. These data are important for physiologically-based PK (PBPK) modeling of first-pass metabolism of UGT2B17 substrates.

Testosterone also undergoes metabolism by several other enzymes such as steroid 5 alpha-reductase 2 (SRD5A2), cytochrome P450 3A4 (CYP3A4), 17β-hydroxysteroid dehydrogenase 2 (17βHSD2), and sulfotransferase 2A1 (SULT2A1) [27]. Particularly, CYP3A4, 17βHSD2, and SULT2A1 are expressed both in liver and intestine [28–31]. Our recent clinical study confirmed high circulating levels of glucuronides of androsterone, testosterone and eticholanolone after oral administration of testosterone [32]. However, individual contributions of liver and intestine in formation of these metabolites and their relative significance have not been studied to date. We therefore investigated quantitative metabolite profiling in human hepatocytes and enterocytes after testosterone incubation. Characterization of UGT2B17 contribution and testosterone glucuronidation in the first-pass organs may lead to opportunities in improved and precise oral TRT regimens that may mitigate risks and maximize benefits.

2. Materials and methods

2.1. Chemicals and reagents

Testosterone, alamethicin, UDP-glucuronic acid (UDPGA), magnesium chloride, dibasic and monobasic potassium phosphate were purchased from Sigma-Aldrich (St. Louis, MO). Oxazepam was purchased from Fischer Scientific (Fair Lawn, NJ), and tyrosine kinase inhibitors (TKIs) were kindly provided by Genentech (San Francisco, CA). Testosterone metabolites, respective conjugates, and standards were purchased from Cerilliant Corporation (Round Rock, TX) and Steraloid (Newport, RI). Bovine serum albumin (BSA) and protein extraction reagents were obtained from Thermo Fisher Scientific (Rockford, IL). Protein quantification chemicals and reagents were obtained as previously reported [33]. Hepatocyte thawing (MCHT50) and incubation (MM250) media were obtained from Lonza (Durham, NC), whereas, enterocytes thawing (CERM) and incubation (HQM) media were from IVAL (Columbia, MD). Synthetic light (with amino acid analysis) and heavy labeled

peptides were purchased from New England Peptides (Boston, MA) and Thermo Fisher Scientific (Rockford, IL), respectively.

2.2. Procurement of human liver and intestinal cells and subcellular fractions

Cryopreserved primary human hepatocytes (n=5) and enterocytes (n=16) were obtained from Lonza (Durham, NC) and IVAL (Columbia, MD), respectively. Pooled human microsomes (HLM), intestinal microsomes (HIM), liver S9 and intestinal S9 fractions were obtained from Xenotech (Kansas City, KS). HLMs (n=26) from individual donors were procured from the University of Washington School of Pharmacy Liver Bank (Seattle, WA) with institutional review board (IRB) reviewed to be exempt from further IRB-approval. Proteomics, activity, and genotyping data were previously published [2]; a subset of adult samples were used for reproduction at differing concentrations of testosterone . Donor-matched intestinal tissue segments (n=6) were procured from Pomeranian Medical University, Szczecin, Poland, and approved by the local Bioethics Committee. Sample demographics are described in Table 1.

2.3. Microsome isolation from donor-matched intestinal sections

Donor-matched HIMs were isolated from different sections of intestine, i.e., duodenum (D), jejunum (J1–J3, three sections), ileum (I), and colon (C), from six individual donors. Tissue samples were disrupted using cell crusher paddles in liquid-nitrogen and HIMs were isolated using protocols from Microsome isolation kit (Abcam, Cambridge, United Kingdom) described elsewhere [34]. Total protein was determined by bicinchoninic acid (BCA) assay using the Pierce BCA Protein Assay Kit (Thermo Fisher Scientific, Rockford, IL) per manufacturer's protocol.

2.4. Membrane protein extraction from primary cells and total protein quantification

Membrane proteins were extracted from the cells using Mem-PER Plus Membrane Protein Extraction kit protocol (Rockford, IL). Briefly, previously washed and frozen hepatocytes (0.7 to 6 million) and enterocytes (6.7–37 million) were resuspended with permeabilization buffer (200 or 400 μL), gently mixed, and incubated on a Compact Digital Waving Rotator (Thermo Fisher Scientific, Rockford, IL) for 30 minutes (4°C) at 300 rpm. Permeabilized cells were centrifuged at 16,000g for 15 minutes (4°C), and resulting supernatant containing cytosolic proteins was removed. Remaining pellet was resuspended with equivolume solubilization buffer, gently mixed, incubated for 60 minutes at 300 rpm (4°C), and centrifuged at 16,000g for 15 minutes (4°C). Resulting supernatant containing membrane proteins was collected and total protein quantification was measured with BCA assay (Thermo Fisher Scientific, Rockford, IL). Remaining solubilized membrane fraction was stored at −80°C for subsequent digestion and LC-MS/MS analysis.

2.5. Protein denaturation, reduction, alkylation, enrichment and trypsin digestion

Trypsin digestion was performed as previously described [33] for HLM and cell membrane samples. In brief, 10 μL dithiothreitol (250 mM), 30 μL ammonium bicarbonate buffer (100 mM, pH 7.8), 20 μL BSA (0.02 mg/mL), and 10 μL human serum albumin (10 mg/mL) were added to 80 μL samples (≤ 2 mg/mL total protein), followed by heat denaturation and

reduction for 10 minutes at 95°C. Upon cooling to room temperature, alkylation was performed by addition of 20 μL iodoacetamide (500 mM) and incubation in room temperature (in dark) for 30 minutes. Protein enrichment and desalting was done with extraction using chloroform-methanol-water (1:5:4) and resulting pellet washed and resuspended in 60 μL ammonium bicarbonate buffer (50 mM, pH 7.8). Trypsin (0.16 μg/μL) was added for digestion for 16 hours at 300 rpm (37°C). Digestion was quenched on dry ice with addition of 20 μL of heavy peptide internal standard cocktail and 10 μl acetonitrile: water 80:20 (v/v) with 0.5% formic acid. After centrifugation at 4000g for 5 minutes (4°C), resulting supernatant was analyzed by LC-MS/MS method.

UGT2B17 quantification in donor-matched individual HIMs was performed at a different site (Oswald lab, University of Greifswald, Greifswald, Germany) using a slightly different method. The differences include trypsin digestion by filter-aided sample preparation (FASP) protocol and the use of ProteaseMax (Promega, Madison, WI) as a surfactant as discussed in detail elsewhere [35]. Three quality control HLM samples previously characterized for UGT2B17 abundance using method described above were used as quality controls for FASP protocol to address inter-laboratory technical variability.

2.6. Quantification of Surrogate peptides of UGT2B17 and UGT2B15 in subcellular fractions

HLM, S9 fractions, and hepatocyte cell membranes were analyzed using Sciex Triple Quadrupole 6500 system (Sciex, Framingham, MA) coupled to Acquity UPLC System (Waters Technologies, Milford, MA). Chromatographic separation of peptides was achieved on ACQUITY UPLC HSS T3 1.8 μm, C_{18} 100A; 100 × 2.1 mm (Waters, Milford, MA) column. Skyline and Analyst 1.6.2 software were used to process acquired LC-MS/MS data. Detailed LC-MS/MS parameters have been previously published [2]. To address technical variability, we used heavy peptide internal standard as well as BSA for exogenous protein standard for all samples except enterocytes due to preexistence of BSA.

For donor-matched HIMs and three quality control samples digested using FASP protocol, LC-MS/MS analysis was performed using Kinetex C18 reverse phase column (100 x 2.1 mm, Phenomenex, Torrance, CA) and AB Sciex QTRAP 5500 system (Sciex, Framingham, MA). Data analysis was done using MultiQuant 3.0.2 software (Sciex, Framingham, MA). As individual HIM samples were quantified using FASP protocol, three HLM samples representing deletion, mid and high UGT2B17 abundance were used as quality controls and calibrators to address any technical variability.

2.7. Testosterone glucuronidation assay in subcellular fractions

Testosterone glucuronidation assay was performed in individual and pooled microsomes and S9 fractions except donor-matched HIMs due to limited samples. Assays were performed in triplicates with 10 μg of protein in 5 mM $MgCl_2$ and 100 mM potassium phosphate buffer (pH 7.4), 0.01% BSA, and 0.1 mg/mL of alamethicin in 100 μL final volume with testosterone (50 nM to 5 μM). After 15 minutes of pretreatment on ice, reactions were initiated by addition of 2.5 mM UDP-glucuronic acid (UDPGA), incubated for 30 minutes (37°C) at 300 rpm, and terminated using 200 μL of ice-cold acetonitrile containing

deuterated TG or rosuvastatin as validated internal standards. Samples were centrifuged at 10,000g for 5 minutes (4°C). TG (Table 2) and rosuvastatin (*m/z* 482.1→258.2; DP 70; CE 40) were quantified in supernatant by LC-MS/MS. Enzyme kinetic parameters (Vmax and Km) were determined for UGT2B17 using three HLMs with high, mid, or null UGT2B17 abundance (9.7, 2.3, and 0.06 pmol/mg microsomal protein, respectively) with comparable UGT2B15 abundance (27, 20, and 34 pmol/mg microsomal protein, respectively). Assays were performed in triplicates with varying testosterone concentrations (0.05, 0.25, 0.5, 2.5, 5, 10, 15, 25 μM) and closely followed the protocol for testosterone glucuronidation assay.

2.8. Inhibition of UGT2B17 activity by tyrosine kinase inhibitors in HLM

UGT2B17 inhibition assays were performed on two HLMs expressing high and below limit of detection (LOD) UGT2B17 abundance (9.7 and 0.06 pmol/mg microsomal protein) with comparable UGT2B15 abundance (27 and 24 pmol/mg microsomal protein). Inhibition assays were performed in triplicates and followed the testosterone glucuronidation assay. One and 25 μM of various TKIs (gefitinib, lapatinib, pazopanib, sorafenib, sunitinib, sirolimus, temsirolimus, dasatinib, nilotinib, and imatinib) were preincubated for 5 minutes at 37°C prior to reaction initiation with UDPGA with 5 μM testosterone to screen for UGT2B17 specificity. The most potent and selective UGT2B17 inhibitor imatinib was further assayed for IC_{50} determination with varying imatinib concentrations (0.01, 0.02, 0.05, 0.1, 0.5, 1, 10, 50, and 100 μM). UGT2B17 activity was measured with TG formation with 1 μM testosterone. Oxazepam was used as a probe substrate for UGT2B15 activity by measuring oxazepam glucuronide formation (*m/z* 463.3→287.1, 269.1; DP 70; CE 20) with 10 μM oxazepam.

2.9. Testosterone metabolism in human hepatocytes and enterocytes

Hepatocytes (n=5) were thawed for 90 to 120 seconds in 37°C waterbath, resuspended in 15 mL of MCHT50, and centrifuged at 100g for 8 minutes at room temperature. Cell count was performed using Nexcelom Bioscience Cellometer Auto T4 (Lawrence, MA), followed by a second centrifugation at 100g for 1 minute. Cells were then resuspended in MM250 at 1 million cells per mL concentration and preincubated for 10 minutes at 37°C. Reactions were initiated by adding 500 μL of hepatocyte suspension to 500 μL pre-warmed MM250 containing 100 μM Testosterone in 12-well plates. Final 1 mL mixture in each well contained 0.5 million cells in 50 μM Testosterone, which was incubated for 60 minutes (37°C) at 100 rpm. Total organic solvent (v/v) did not exceed 0.1%. Incubation was terminated by addition of 2 mL ice-cold acetonitrile containing internal standards. Cells were mechanically lysed by vortex mixing and centrifugation at 3000g for 10 minutes (4°C). Supernatant was immediately stored at −80°C prior to analysis by LC-MS/MS. Enterocytes (n=16) followed a similar protocol using CERM and HQM as thawing and incubation media, respectively, and were seeded to yield a final 100 μL mixture in 96-well plate containing up to 150,000 cells in 50 μM Testosterone followed by a 120-minute incubation (37°C) at 100 rpm.

2.10. LC-MS/MS analysis of testosterone metabolites formed in human hepatocytes and enterocytes

Testosterone and its metabolites (Table 2) were measured by LC-MS/MS using the same system as protein quantification. Quantified metabolites include testosterone glucuronide (TG), 5α-dihydrotestosterone (DHT), DHT glucuronide (DHTG), androsterone (A), androsterone glucuronide (AG), androstenedione (AED), 6-hydroxy testosterone (6OHT), eticholanolone (E), and eticholanolone glucuronide (EG). LC conditions were set at 0.3 mL/min flow rate and 5 μL injection volume with mobile phase A: water with 0.1% formic acid and B: acetonitrile with 0.1% formic acid. The gradient program was: 85% A (0–2.5 min), 85-60% (2.5–8.5 min), 60-50% (8.5–12.8 min), 50-2% (12.8–13 min), 2–85% (13–15 min). Whenever available, deuterated internal standards were used. Lower limit of quantification (LLOQ) was established, with limit of detection (LOD) set as one-third of LLOQ values. Multiple reaction monitoring (MRM) parameters used to quantify testosterone metabolites are shown in Table 2.

2.11. Data Analysis

2.11.1. Fractional contribution of UGT2B17 in testosterone metabolism in HLM

—Fractional contribution (f_m) of UGT2B17 was calculated using Equation 1 through 3. We assumed thatactivity measured by TG formation (CL) is mediated only by UGT2B17 and UGT2B15. Thus all TG formation was via UGT2B15 in homozygous UGT2B17 gene deletion samples (UGT2B17 del-del). Normalized average UGT2B15 activity was calculated as the average activity in these samples divided by their average UGT2B15 protein expression (Equation 1). We then obtained individual UGT2B15 activity by multiplying average UGT2B15 activity with individual UGT2B15 protein abundance. This value is subtracted from total individual activity ($CL_{total\ obs}$) to acquire individual UGT2B17 activity ($CL_{UGT2B17}$) (Equation 2). Individual UGT2B15 and UGT2B17 f_m are the respective individual activities divided by total individual TG formation (Equation 3). Negative estimates of UGT2B17 activity were adjusted to zero. Calculations were performed using Microsoft Excel (Redmond, WA).

$$\text{Avg}\,CL_{UGT2B15} = \frac{\text{Mean}\,CL_{UGT_2B_{15}}(\text{UGT2B17 del} - \text{del})}{\text{Mean}\,[E]_{UGT_2B_{15}}(\text{UGT2B17 del} - \text{del})} \quad (1)$$

$$CL_{UGT2B17} = CL_{total\ obs} - \text{Avg}CL_{UGT2B15} * [E]_{UGT2B15} \quad (2)$$

$$f_{m,\,UGT2B17} = CL_{UGT2B17}/CL_{total\ obs} \quad (3)$$

2.11.2. Determination of UGT kinetic parameters—

Enzyme kinetic parameters (K_m and V_{max}) were obtained by fitting the Michaelis-Menten equation using GraphPad Prism

version 5.03 for Windows (La Jolla, CA) (Equation 4), where Y is testosterone glucuronidation rate (pmol/mg protein/min) and X is testosterone concentration (μM).

$$Y = \frac{V_{max} * X}{(K_m + X)} \quad (4)$$

2.11.3. IC50 calculation for imatinib—IC_{50} values were calculated using the following nonlinear regression model (Equation 5), where Y is relative glucuronidation activity (% TG formation) and X is inhibitor concentration (μM). IC_{50} values were obtained using GraphPad Prism version 5.03 for Windows (La Jolla, CA).

$$Y = \frac{100}{(1 + \frac{X}{IC_{50}})} \quad (5)$$

2.12. Statistical Analysis

UGT2B217 protein abundance between HLM and HIM (excluding colon) was compared using Mann-Whitney test. UGT2B17 protein abundance-TG formation correlation and corresponding p-values were obtained using Spearman's correlation. Statistical analyses were performed with GraphPad Prism version 5.03 for Windows (La Jolla, CA).

3. Results

3.1. UGT2B17 and UGT2B15 abundance and correlation with testosterone glucuronidation in human liver and intestinal subcellular fractions

Protein abundance in adult HLMs (n=26) showed high inter-individual variability for UGT2B17 (>160-fold) with 46% (n=12) falling below LLOQ, which included 23% confirmed gene deletions (n=6) (Table 3), while UGT2B15 protein abundance was much less variable (4-fold) (Figure 1A). High variability in UGT2B17 was also observed in HIMs (>492-fold), with an increasing trend observed down the gastrointestinal (GI) segments (Figure 1C). Average UGT2B17 protein abundance in the HIM (excluding colon) was significantly higher (4.4-fold) than HLM (p=0.016). UGT2B15 was not detectable in donor-matched HIMs and pooled fractions, in agreement with published literature [26,35,36]. . UGT2B17 protein abundance in individual HLM showed a strong correlation with testosterone glucuronidation activity (r^2= 0.77, p<0.001) (Figure 1E), confirming its major role in TG formation. UGT2B15 showed a significant correlation with TG formation only in samples with UGT2B17 level below LLOQ (r^2=0.65, p=0.02) (Figure 1F), consistent with our previous findings [2]. In addition, UGT2B17 abundance and TG formation was higher in pooled subcellular fractions from intestine compared to liver (Figure 1F). Estimated fractional contribution for UGT2B17 ($f_{m,UGT2B17}$) and UGT2B15 ($f_{m,UGT2B15}$) ranged from 0 to 0.91, and 0.09 to 1, respectively, depending on UGT2B17 variability (Figure 1B). For example, $f_{m,UGT2B17}$ was 0.74 or higher in samples with UGT2B17 abundance >1 pmol/mg

microsomal protein, whereas, $f_{m,UGT2B15}$ was 0.85 or higher in samples that were below LLOQ for UGT2B17.

3.2. Enzyme kinetic parameters for testosterone in HLM

Calculated K_m (μM) and V_{max} (pmol/mg protein/min) for high, mid, and null UGT2B17-expressing HLMs were 13.5, 4.0, and 8.1 μM, and 5.96, 1.44, and 0.295 nmol/mg protein/min, respectively (Figure 2A). High and mid UGT2B17-expressing HLMs had a 4-fold difference in absolute UGT2B17 protein abundance (9.6 and 2.3 pmol/mg protein, respectively) with a corresponding 4-fold difference in calculated V_{max}. Noticeable substrate depletion was observed for high UGT2B17 expressing HLM at low and mid testosterone concentration ranges, perhaps leading to variability observed in K_m values.

3.3. Inhibition of UGT2B17 and UGT2B15 by Tyrosine Kinase Inhibitors

Among the 10 TKIs screened for UGT2B17 inhibition, imatinib was the most potent and selective inhibitor for UGT2B17 (Figure 2D). IC_{50} values for imatinib using testosterone as a substrate was 0.31 μM for high-UGT2B17 expressing HLM and 69 μM for low-UGT2B17 expressing HLM (Figure 2B), with the lower value being in agreement with published literature for recombinant UGT2B17 [37]. When oxazepam was used as a probe substrate for UGT2B15, imatinib IC_{50} values in high- and low-UGT2B17 expressing HLM were similar with mean values of 54 μM and 79 μM, respectively (Figure 2C).

3.4. UGT2B17 and UGT2B15 protein abundance and testosterone metabolism in primary human hepatocytes and enterocytes

In hepatocytes, protein abundance (mean ± SD, pmol/mg membrane protein) for UGT2B17 and UGT2B15 were 0.4 ± 0.4 and 6.5 ± 4.3, respectively. In enterocytes, UGT2B17 protein abundance (mean ± SD, fmol/million cells) was 11.8 ± 12.6 and UGT2B15 was not detected.

Structures of quantified testosterone metabolites with corresponding enzymes in a simplified metabolism scheme are shown in Figure 3A, with respective metabolite formation rates of each metabolite listed in Table 4. A representative chromatogram of a hepatocyte incubation showing chromatographic and MS/MS separation is shown in Figure 3B. The three most abundant metabolites were AED, TG, and 6OH for both hepatocytes and enterocytes, whereas, DHT, DHTG, A, and AG combined constituted less than 4% (hepatocytes) and 1% (enterocytes), and E and EG were below LLOQ (Figures 4A, 4C). TG was the second major metabolite measured, at two-fold or higher abundance levels compared to other metabolites except AED. TG formation rate (mean ± SD, pmol/million cells/hour) was higher in hepatocytes (4836 ± 2460) compared to enterocytes (437 ± 433). Correlation between relative UGT2B17 protein abundance and TG formation was significant in enterocytes (r^2=0.68, p=0.004). However, the correlation was not significant in hepatocytes, perhaps due to smaller sample size and confounding role of UGT2B15 (Figures 4B, 4D). UGT2B15 also showed nonsignificant correlation with TG formation in hepatocytes and was not detected in enterocytes.

4. Discussion

To the best of our knowledge, this is the first study to demonstrate regional distribution of UGT2B17 in paired intestinal microsomes. It is also the first to apply a primary enterocyte model to study testosterone metabolomics and UGT activity in enterocytes in comparison with hepatocytes. Here we also propose a facile method of f_m estimation for UGT2B17 substrates in HLMs using gene deletion samples when two or more UGT isoforms are involved in glucuronidation.

UGT2B17 protein abundance in subcellular fractions revealed two findings with notable implications. First, UGT2B17 showed 4.4-fold higher abundance in intestine compared to liver, in agreement with published literature reporting two-fold higher levels of UGT2B17 in intestine [26]. The same article reports UGT2B17 constituting 3% of total UGT isoforms in the liver but 59% in the intestine, in contrast to UGT2B15 which has high relative hepatic expression of 12% but was undetected in intestine, similar to our findings. Again in contrast to UGT2B17, UGT2B7, which is considered to be a major drug-metabolizing UGT isoform [38], constitutes 22% and 4% of total UGT isoforms in the liver and intestine, respectively [26]. This unique expression of UGT2B17 augments the clinical significance of first pass metabolism for orally administered UGT2B17 substrates. Bioavailability (F) is a product of fraction absorbed (F_a), fraction escaping intestinal metabolism (F_g), and fraction escaping hepatic metabolism (F_h). In general, intestinal metabolism is considered to be equal to or lower than liver due to lower DME expression and activity in the GI wall [28,39,40]. However, for UGT2B17 substrates, significantly greater intestinal metabolism may occur relative to other UGTs, resulting in lower F_g than F_h, leading to a highly variable first-pass effect with less variable systemic clearance. An example of this is MK-7246, which was discontinued from development due to unexpected PK variability. This was later attributed to UGT2B17, showing a 25-fold higher area under the curve in subjects with UGT2B17 gene deletion [41]. Secondly, UGT2B17 showed an increasing trend down the GI tract from duodenum to colon. This indicates that the site of absorption may impact the extent of UGT2B17-mediated GI metabolism (F_g), which can potential contribute to significant variability in drug disposition due to factors affecting GI motility and transit time and may also be viable for targeted drug delivery. It also brings in likelihood of variability in drug disposition by affecting the extent of enterohepatic recycling. On the other hand, UGT2B15 showed relatively consistent expression in the liver and was undetected in pooled intestinal subcellular fractions and cells. This supports the absence of UGT2B15 in intestinal tissues, where literature reports detection at mRNA levels and inconsistency at protein levels [26,36,42].

Considering the higher expression of UGT2B17 in HIM, it is reasonable to expect more TG formation in enterocytes compared to hepatocytes. However, enterocytes showed an overall 10-fold lower activity, despite the metabolome profile being reflective of hepatocytes. This is possibly due to lower soluble protein content of enterocytes and loss of activity during cryopreservation of enterocytes. There have been two published studies reporting cryopreserved enterocyte activities [43,44] and further characterization would be beneficial.

The estimation method for fractional contribution is applicable to other polymorphic enzymes such as CYP2D6. The wide range of $f_{m,UGT2B17}$ from 0 to 0.91 shows variable DDI potentials for UGT2B17-specific substrates, which is highlighted by imatinib as a potent UGT2B17-specific inhibitor. Imatinib IC_{50} value of 0.3 μM, combined with calculated maximum unbound hepatic input concentration of 0.7 μM [37], can lead to double the exposure of a UGT2B17-specific substrate. However, the magnitude of imatinib inhibition will vary widely depending on UGT2B17 protein abundance levels thus $f_{m,UGT2B17}$. For the subset of high UGT2B17-expressors, potential DDIs become particularly concerning, where UGT2B17 inhibition will lead to dramatic increase in its substrate. However, identification of these high-expressors cannot easily be done, as genotype, age, sex, and SNP combined accounts for only 29% of UGT2B17 variability [2]. Thus, identifying a phenotypic biomarker or probe drug for UGT2B17 would be beneficial in identifying these individuals at high risk for DDI.

Androstenedione (AED), rather than TG as a major metabolite in both hepatocytes and enterocytes is an unexpected, albeit reasonable finding. 17 β-HSD2 mediates AED formation from testosterone, while 17 β-HSD1,17 β-HSD3, and 17 β-HSD5 convert AED to testosterone [29]. 17 β-HSD2 has high expression in GI and liver, while 17 β-HSD1 and 17 β-HSD3 are sex tissue-specific, and 17 β-HSD5 is ubiquitously expressed [45,46]. AED is one of the main adrenal hormones in circulation along with DHEA as an inactive adrenal precursor. AED as a reservoir pool explains the preferential AED formation over elimination via glucuronidation pathway at supra-physiological testosterone concentrations in a limited timeframe.

Figure 5 shows the average plasma metabolite profile in seven healthy adult men at baseline (Figure 5A), following an 800mg oral testosterone administration up to 24 hours after chemical castration with acyline (Figure 5B), and the fold-difference from baseline (Figure 5C) from a previously published study [32]. TG had the most significant increase in percentage and absolute concentration (10-fold and 280-fold, respectively), compared to the next highest increase seen in DHTG and EG (both about 1.5-fold and 40-fold, respectively). This indicates the important role of glucuronidation in exogenous testosterone elimination, which may have been attenuated by AED formation in the cell systems.

There are several limitations of this study, a major limitation being small sample sizes. In addition, while we could detect most of the testosterone metabolites, we were unable to quantify all known and intermediate metabolites, such as 6OH glucuronide, testosterone sulfate, androstanedione, and estradiol. Having this information would present a more comprehensive picture of testosterone metabolism. In addition, the *in vitro* enterocyte cell system that was used has not been extensively validated, although exhibited metabolic activity [43]. Moreover, restrictions in incubation times may result in incomplete reflection of *in vivo* metabolism that encompass sequential reactions.

In summary, we characterized UGT2B17 in first-pass effect organs, whose role in drug metabolism remains understudied and underappreciated. For example, while one study showed UGT2B17 to be one of the main isoforms responsible for clopidogrel acyl glucuronide (CAG) formation [47], another study did not include this isoform and hence

concluded that UGT2B7 forms CAG [48]. In addition, TRT has recently come under scrutiny due to reports of possible increased cardiovascular events, and the risks and benefits of TRT still remain contentious among practitioners [14,49–51]. As TRT use continues to increase, elucidation of the testosterone elimination pathways is crucial for individualized dosing and optimizing treatment in precise TRT. Our data on UGT2B17 abundance will be applicable in building a PBPK model for first-pass metabolism for UGT2B17 substrates including testosterone. Extensive research and literature exist on testosterone biosynthesis pathways, but data on exogenous testosterone metabolism and elimination pathways are still lacking.

Acknowledgments

This work was supported by the National Institutes of Health (NIH) grant (R01 HD081299) and Department of Pharmaceutics, University of Washington.

References

1. Xue Y, Sun D, Daly A, Yang F, Zhou X, Zhao M, Huang N, Zerjal T, Lee C, Carter NP, Hurles ME, Tyler-Smith C. Adaptive evolution of UGT2B17 copy-number variation. Am J Hum Genet. 2008; 83:337–346. DOI: 10.1016/j.ajhg.2008.08.004 [PubMed: 18760392]
2. Bhatt DK, Basit A, Zhang H, Gaedigk A, Lee S, Claw KG, Mehrotra A, Chaudhry AS, Pearce RE, Gaedigk R, Broeckel U, Thornton TA, Nickerson DA, Schuetz EG, Amory J, Leeder JS, Prasad B. Hepatic Abundance and Activity of Androgen and Drug Metabolizing Enzyme, UGT2B17, are Associated with Genotype. Age, and Sex, Drug Metab Dispos. 2018; dmd.118.080952. doi: 10.1124/dmd.118.080952
3. Wong NS, Seah EZ, Wang LZ, Yeo WL, Yap HL, Chuah B, Lim YW, Ang PC, Tai BC, Lim R, Goh BC, Lee SC. Impact of UDP-gluconoryltransferase 2B17 genotype on vorinostat metabolism and clinical outcomes in Asian women with breast cancer. Pharmacogenet Genomics. 2011; 21:760–768. DOI: 10.1097/FPC.0b013e32834a8639 [PubMed: 21849928]
4. Luo S, Chen G, Truica C, Baird CC, Leitzel K, Lazarus P. Role of the UGT2B17 deletion in exemestane pharmacogenetics. Pharmacogenomics J. 2017; doi: 10.1038/tpj.2017.18
5. Chen G, Luo S, Kozlovich S, Lazarus P. Association between Glucuronidation Genotypes and Urinary NNAL Metabolic Phenotypes in Smokers. Cancer Epidemiol Biomarkers Prev. 2016; 25:1175–1184. DOI: 10.1158/1055-9965.EPI-15-1245 [PubMed: 27197298]
6. Yang TL, Chen XD, Guo Y, Lei SF, Wang JT, Zhou Q, Pan F, Chen Y, Zhang ZX, Dong SS, Xu XH, Yan H, Liu X, Qiu C, Zhu XZ, Chen T, Li M, Zhang H, Zhang L, Drees BM, Hamilton JJ, Papasian CJ, Recker RR, Song XP, Cheng J, Deng HW. Genome-wide copy-number-variation study identified a susceptibility gene, UGT2B17, for osteoporosis. Am J Hum Genet. 2008; 83:663–674. DOI: 10.1016/j.ajhg.2008.10.006 [PubMed: 18992858]
7. Jakobsson J, Ekström L, Inotsume N, Garle M, Lorentzon M, Ohlsson C, Roh HK, Carlström K, Rane A. Large differences in testosterone excretion in Korean and Swedish men are strongly associated with a UDP-glucuronosyl transferase 2B17 polymorphism. J Clin Endocrinol Metab. 2006; 91:687–693. DOI: 10.1210/jc.2005-1643 [PubMed: 16332934]
8. Schulze JJ, Lundmark J, Garle M, Skilving I, Ekström L, Rane A. Doping test results dependent on genotype of uridine diphospho-glucuronosyl transferase 2B17, the major enzyme for testosterone glucuronidation. J Clin Endocrinol Metab. 2008; 93:2500–2506. DOI: 10.1210/jc.2008-0218 [PubMed: 18334593]
9. Zhu AZ, Cox LS, Ahluwalia JS, Renner CC, Hatsukami DK, Benowitz NL, Tyndale RF. Genetic and phenotypic variation in UGT2B17, a testosterone-metabolizing enzyme, is associated with BMI in males. Pharmacogenet Genomics. 2015; 25:263–269. DOI: 10.1097/FPC.0000000000000135 [PubMed: 25794161]
10. Swanson C, Mellström D, Lorentzon M, Vandenput L, Jakobsson J, Rane A, Karlsson M, Ljunggren O, Smith U, Eriksson AL, Bélanger A, Labrie F, Ohlsson C. The uridine diphosphate

glucuronosyltransferase 2B15 D85Y and 2B17 deletion polymorphisms predict the glucuronidation pattern of androgens and fat mass in men. J Clin Endocrinol Metab. 2007; 92:4878–4882. DOI: 10.1210/jc.2007-0359 [PubMed: 17698910]

11. Chew S, Mullin BH, Lewis JR, Spector TD, Prince RL, Wilson SG. Homozygous deletion of the UGT2B17 gene is not associated with osteoporosis risk in elderly Caucasian women. Osteoporos Int. 2011; 22:1981–1986. DOI: 10.1007/s00198-010-1405-0 [PubMed: 20878390]
12. Cai L, Huang W, Chou KC. Prostate cancer with variants in CYP17 and UGT2B17 genes: a meta-analysis. Protein Pept Lett. 2012; 19:62–69. https://www.ncbi.nlm.nih.gov/pubmed/21919858. [PubMed: 21919858]
13. Kpoghomou MA, Soatiana JE, Kalembo FW, Bishwajit G, Sheng W. UGT2B17 Polymorphism and Risk of Prostate Cancer: A Meta-Analysis. ISRN Oncol. 2013; 2013:465916.doi: 10.1155/2013/465916 [PubMed: 24106614]
14. Cheetham TC, An J, Jacobsen SJ, Niu F, Sidney S, Quesenberry CP, VanDenEeden SK. Association of Testosterone Replacement With Cardiovascular Outcomes Among Men With Androgen Deficiency. JAMA Intern Med. 2017; 177:491.doi: 10.1001/jamainternmed.2016.9546 [PubMed: 28241244]
15. Shoskes JJ, Wilson MK, Spinner ML. Pharmacology of testosterone replacement therapy preparations. Transl Androl Urol. 2016; 5:834–843. DOI: 10.21037/tau.2016.07.10 [PubMed: 28078214]
16. Pavlatos AM, Fultz O, Monberg MJ, Vootkur A. Pharmd, Review of oxymetholone: a 17alpha-alkylated anabolic-androgenic steroid. Clin Ther. 2001; 23:789–801. [accessed June 5, 2018] discussion 771. http://www.ncbi.nlm.nih.gov/pubmed/11440282. [PubMed: 11440282]
17. Westaby D, Ogle SJ, Paradinas FJ, Randell JB, Murray-Lyon IM. Liver damage from long-term methyltestosterone. Lancet (London, England). 1977; 2:262–3. [accessed June 5, 2018] http://www.ncbi.nlm.nih.gov/pubmed/69876.
18. Morales A, Bella AJ, Chun S, Lee J, Assimakopoulos P, Bebb R, Gottesman I, Alarie P, Dugré H, Elliott S. A practical guide to diagnosis, management and treatment of testosterone deficiency for Canadian physicians. Can Urol Assoc J. 2010; 4:269–75. [accessed June 7, 2018] http://www.ncbi.nlm.nih.gov/pubmed/20694106. [PubMed: 20694106]
19. Gooren LJ. A ten-year safety study of the oral androgen testosterone undecanoate. J Androl. n.d; 15:212–5. [accessed June 5, 2018] http://www.ncbi.nlm.nih.gov/pubmed/7928661. [PubMed: 7928661]
20. Nieschlag E, Mauss J, Coert A, Kićović P. Plasma androgen levels in men after oral administration of testosterone or testosterone undecanoate. Acta Endocrinol (Copenh). 1975; 79:366–74. [accessed June 5, 2018] http://www.ncbi.nlm.nih.gov/pubmed/1173495. [PubMed: 1173495]
21. Franchimont P, Kicovic PM, Mattei A, Roulier R. Effects of oral testosterone undecanoate in hypogonadal male patients. Clin Endocrinol (Oxf). 1978; 9:313–20. [accessed June 5, 2018] http://www.ncbi.nlm.nih.gov/pubmed/102469. [PubMed: 102469]
22. Daggett PR, Wheeler MJ, Nabarro JD. Oral testosterone, a reappraisal. Horm Res. 1978; 9:121–9. DOI: 10.1159/000178904 [PubMed: 640576]
23. Täuber U, Schröder K, Düsterberg B, Matthes H. Absolute bioavailability of testosterone after oral administration of testosterone-undecanoate and testosterone. Eur J Drug Metab Pharmacokinet. n.d; 11:145–9. [accessed May 16, 2018] http://www.ncbi.nlm.nih.gov/pubmed/3770015. [PubMed: 3770015]
24. SANDBERG AA, SLAUNWHITE WR. Metabolism of 4-C14-testosterone in human subjects. I. Distribution in bile, blood, feces and urine. J Clin Invest. 1956; 35:1331–9. DOI: 10.1172/JCI103389 [PubMed: 13385331]
25. Barbier O, Bélanger A. Inactivation of androgens by UDP-glucuronosyltransferases in the human prostate. Best Pr Res Clin Endocrinol Metab. 2008; 22:259–270. DOI: 10.1016/j.beem.2008.01.001
26. Sato Y, Nagata M, Tetsuka K, Tamura K, Miyashita A, Kawamura A, Usui T. Optimized methods for targeted peptide-based quantification of human uridine 5'-diphosphate-glucuronosyltransferases in biological specimens using liquid chromatography-tandem mass

spectrometry. Drug Metab Dispos. 2014; 42:885–9. DOI: 10.1124/dmd.113.056291 [PubMed: 24595681]

27. Schiffer L, Arlt W, Storbeck KH. Intracrine androgen biosynthesis, metabolism and action revisited. Mol Cell Endocrinol. 2017; doi: 10.1016/j.mce.2017.08.016
28. Thummel KE. Gut instincts: CYP3A4 and intestinal drug metabolism. J Clin Invest. 2007; 117:3173–6. DOI: 10.1172/JCI34007 [PubMed: 17975661]
29. Sano T, Hirasawa G, Takeyama J, Darnel AD, Suzuki T, Moriya T, Kato K, Sekine H, Ohara S, Shimosegawa T, Nakamura J, Yoshihama M, Harada N, Sasano H. 17 beta-Hydroxysteroid dehydrogenase type 2 expression and enzyme activity in the human gastrointestinal tract. Clin Sci (Lond). 2001; 101:485–91. [accessed January 18, 2018] http://www.ncbi.nlm.nih.gov/pubmed/11672453. [PubMed: 11672453]
30. Riches Z, Stanley EL, Bloomer JC, Coughtrie MWH. Quantitative Evaluation of the Expression and Activity of Five Major Sulfotransferases (SULTs) in Human Tissues: The SULT "Pie". Drug Metab Dispos. 2009; 37:2255–2261. DOI: 10.1124/dmd.109.028399 [PubMed: 19679676]
31. Shin H-CC, Kim H-RR, Cho H-JJ, Yi H, Cho S-MM, Lee D-GG, Abd El-Aty AM, Kim J-SS, Sun D, Amidon GL. Comparative gene expression of intestinal metabolizing enzymes. Biopharm Drug Dispos. 2009; 30:411–421. DOI: 10.1002/bdd.675 [PubMed: 19746353]
32. Basit A, Amory JK, Prasad B. Effect of Dose and 5α-Reductase Inhibition on the Circulating Testosterone Metabolite Profile of Men Administered Oral Testosterone. Clin Transl Sci. 2018; doi: 10.1111/cts.12569
33. Xu M, Bhatt DK, Yeung CK, Claw KG, Chaudhry AS, Gaedigk A, Pearce RE, Broeckel U, Gaedigk R, Nickerson DA, Schuetz E, Rettie AE, Leeder S, Thummel KE, Prasad B, Leeder JS, Thummel KE, Prasad B. Genetic and Non-genetic Factors Associated with Protein Abundance of Flavin-containing Monooxygenase 3 in Human Liver. J Pharmacol Exp Ther. 2017; 363:265–274. DOI: 10.1124/jpet.117.243113 [PubMed: 28819071]
34. Busch D, Fritz A, Partecke LI, Heidecke C-D, Oswald S. LC–MS/MS method for the simultaneous quantification of intestinal CYP and UGT activity. J Pharm Biomed Anal. 2018; 155:194–201. DOI: 10.1016/J.JPBA.2018.04.003 [PubMed: 29649788]
35. Drozdzik M, Busch D, Lapczuk J, Müller J, Ostrowski M, Kurzawski M, Oswald S. Protein Abundance of Clinically Relevant Drug-Metabolizing Enzymes in the Human Liver and Intestine: A Comparative Analysis in Paired Tissue Specimens. Clin Pharmacol Ther. 2017; doi: 10.1002/cpt.967
36. Gröer C, Busch D, Patrzyk M, Beyer K, Busemann A, Heidecke CD, Drozdzik M, Siegmund W, Oswald S. Absolute protein quantification of clinically relevant cytochrome P450 enzymes and UDP-glucuronosyltransferases by mass spectrometry-based targeted proteomics. J Pharm Biomed Anal. 2014; 100:393–401. DOI: 10.1016/J.JPBA.2014.08.016 [PubMed: 25218440]
37. Zhang N, Liu Y, Jeong H. Drug-Drug Interaction Potentials of Tyrosine Kinase Inhibitors via Inhibition of UDP-Glucuronosyltransferases. Sci Rep. 2015; 5:17778.doi: 10.1038/srep17778 [PubMed: 26642944]
38. Oda S, Fukami T, Yokoi T, Nakajima M. A comprehensive review of UDP-glucuronosyltransferase and esterases for drug development. Drug Metab Pharmacokinet. 2015; 30:30–51. DOI: 10.1016/j.dmpk.2014.12.001 [PubMed: 25760529]
39. Shen Kunze. Thummel, Enzyme-catalyzed processes of first-pass hepatic and intestinal drug extraction. Adv Drug Deliv Rev. 1997; 27:99–127. [accessed April 3, 2018] http://www.ncbi.nlm.nih.gov/pubmed/10837554. [PubMed: 10837554]
40. Jones CR, Hatley OJD, Ungell A-L, Hilgendorf C, Peters SA, Rostami-Hodjegan A. Gut Wall Metabolism. Application of Pre-Clinical Models for the Prediction of Human Drug Absorption and First-Pass Elimination. AAPS J. 2016; 18:589–604. DOI: 10.1208/s12248-016-9889-y [PubMed: 26964996]
41. Wang YH, Trucksis M, McElwee JJ, Wong PH, Maciolek C, Thompson CD, Prueksaritanont T, Garrett GC, Declercq R, Vets E, Willson KJ, Smith RC, Klappenbach JA, Opiteck GJ, Tsou JA, Gibson C, Laethem T, Panorchan P, Iwamoto M, Shaw PM, Wagner JA, Harrelson JC. UGT2B17 genetic polymorphisms dramatically affect the pharmacokinetics of MK-7246 in healthy subjects in a first-in-human study. Clin Pharmacol Ther. 2012; 92:96–102. DOI: 10.1038/clpt.2012.20 [PubMed: 22669291]

42. Miyauchi E, Tachikawa M, Declèves X, Uchida Y, Bouillot J-LL, Poitou C, Oppert J-MM, Mouly S, Bergmann J-FF, Terasaki T, Scherrmann J-MM, Lloret-Linares C. Quantitative Atlas of Cytochrome P450, UDP-Glucuronosyltransferase, and Transporter Proteins in Jejunum of Morbidly Obese Subjects. Mol Pharm. 2016; 13:2631–2640. DOI: 10.1021/acs.molpharmaceut.6b00085 [PubMed: 27347605]
43. Ho M-CD, Ring N, Amaral K, Doshi U, Li AP. Human Enterocytes as an In Vitro Model for the Evaluation of Intestinal Drug Metabolism: Characterization of Drug-Metabolizing Enzyme Activities of Cryopreserved Human Enterocytes from Twenty-Four Donors. Drug Metab Dispos. 2017; 45:686–691. DOI: 10.1124/dmd.116.074377 [PubMed: 28396528]
44. Yan Z, Wong S, Kelly J, Le H, Liu N, Kosaka M, Tey S, Vuong P, Li A. Utility of Pooled Cryopreserved Human Enterocytes as An In Vitro Model for Assessing Intestinal Clearance and Drug-Drug Interactions. Drug Metab Lett. 2017; 12doi: 10.2174/1872312812666171213114422
45. Miettinen MM, Mustonen MV, Poutanen MH, Isomaa VV, Vihko RK. Human 17 beta-hydroxysteroid dehydrogenase type 1 and type 2 isoenzymes have opposite activities in cultured cells and characteristic cell- and tissue-specific expression. Biochem J. 1996; 314(Pt 3):839–45. [accessed April 3, 2018] http://www.ncbi.nlm.nih.gov/pubmed/8615778. [PubMed: 8615778]
46. Takeyama J, Suzuki T, Hirasawa G, Muramatsu Y, Nagura H, Iinuma K, Nakamura J, Kimura K, Yoshihama M, Harada N, Andersson S, Sasano H. 17β-Hydroxysteroid Dehydrogenase Type 1 and 2 Expression in the Human Fetus [1]. J Clin Endocrinol Metab. 2000; 85:410–416. DOI: 10.1210/jcem.85.1.6323 [PubMed: 10634418]
47. Kahma H, Filppula AM, Neuvonen M, Tarkiainen EK, Tornio A, Holmberg MT, Itkonen MK, Finel M, Neuvonen PJ, Niemi M, Backman JT. Clopidogrel Carboxylic Acid Glucuronidation is Mediated Mainly by UGT2B7, UGT2B4, and UGT2B17: Implications for Pharmacogenetics and Drug-Drug Interactions. Drug Metab Dispos. 2018; 46:141–150. DOI: 10.1124/dmd.117.078162 [PubMed: 29138287]
48. Ji J-Z, Huang B-B, Gu T-T, Tai T, Zhou H, Jia Y-M, Mi Q-Y, Zhang M-R, Xie H-G. Human UGT2B7 is the major isoform responsible for the glucuronidation of clopidogrel carboxylate. Biopharm Drug Dispos. 2018; doi: 10.1002/bdd.2117
49. Clavell-Hernández J, Wang R. Emerging Evidences in the Long Standing Controversy Regarding Testosterone Replacement Therapy and Cardiovascular Events. World J Mens Health. 2018; 36:92.doi: 10.5534/wjmh.17050 [PubMed: 29706034]
50. Ponce OJ, Spencer-Bonilla G, Alvarez-Villalobos N, Serrano V, Singh-Ospina N, Rodriguez-Gutierrez R, Salcido-Montenegro A, Benkhadra R, Prokop LJ, Bhasin S, Brito JP. The Efficacy and Adverse Events of Testosterone Replacement Therapy in Hypogonadal Men: A Systematic Review and Meta-Analysis of Randomized, Placebo-Controlled Trials. J Clin Endocrinol Metab. 2018; 103:1745–1754. DOI: 10.1210/jc.2018-00404
51. Vigen R, O'Donnell CI, Barón AE, Grunwald GK, Maddox TM, Bradley SM, Barqawi A, Woning G, Wierman ME, Plomondon ME, Rumsfeld JS, Ho PM. Association of testosterone therapy with mortality, myocardial infarction, and stroke in men with low testosterone levels. JAMA. 2013; 310:1829–36. DOI: 10.1001/jama.2013.280386 [PubMed: 24193080]

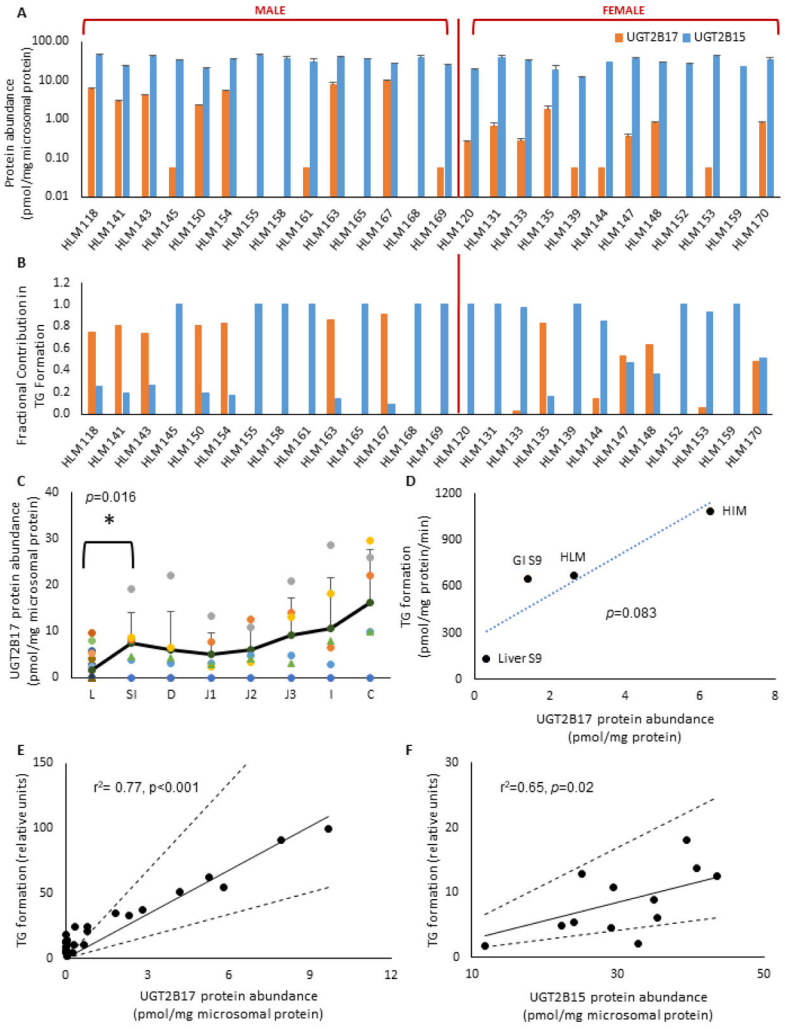

Fig. 1. UGT2B protein abundance and testosterone glucuronidation in human liver and intestinal subcellular fractions

A. UGT2B17 and UGT2B15 protein abundance in HLM (n=26). 21% (n=6) HLM were confirmed UGT2B17 gene deletions (HLM 152, 155, 158, 159, 165, 168); **B.** Estimated fractional contribution (f_m) of UGT2B17 and UGT2B15 in testosterone glucuronidation in HLM (n=26). $f_{m,\ UGT2B17}$ estimates were adjusted to zero for negative values in HLMs with low testosterone glucuronidation activities (n=6). **C.** UGT2B17 protein abundance (pmol/mg microsomal protein) in human liver microsomes (L, n=26) and donor-matched human intestinal microsomes (n=6) shown as average small intestine (SI), duodenum (D), jejunum (J1, J2, J3), ileum (I), and colon (C). Black solid line shows average values for each group. Average UGT2B17 values for L and SI showed statistically significant difference (p=0.016). 46% of HLM (n=12) and 21% of HIM (n=1) were below lower limit of quantification (LLOQ); **D.** Correlation between testosterone glucuronide (TG) formation (pmol/ min/ mg microsomal protein) and UGT2B17 abundance (pmol/mg protein) in human liver and intestinal microsomes and S9 fractions; **E & F.** Correlations between relative testosterone glucuronidation activity in adult HLM and (E) UGT2B17 abundance (n=26) and (F)

UGT2B15 abundance in UGT2B17-LLOQ samples (n=12). Solid and dashed lines depict expected and two-fold range values for perfect correlation, respectively.

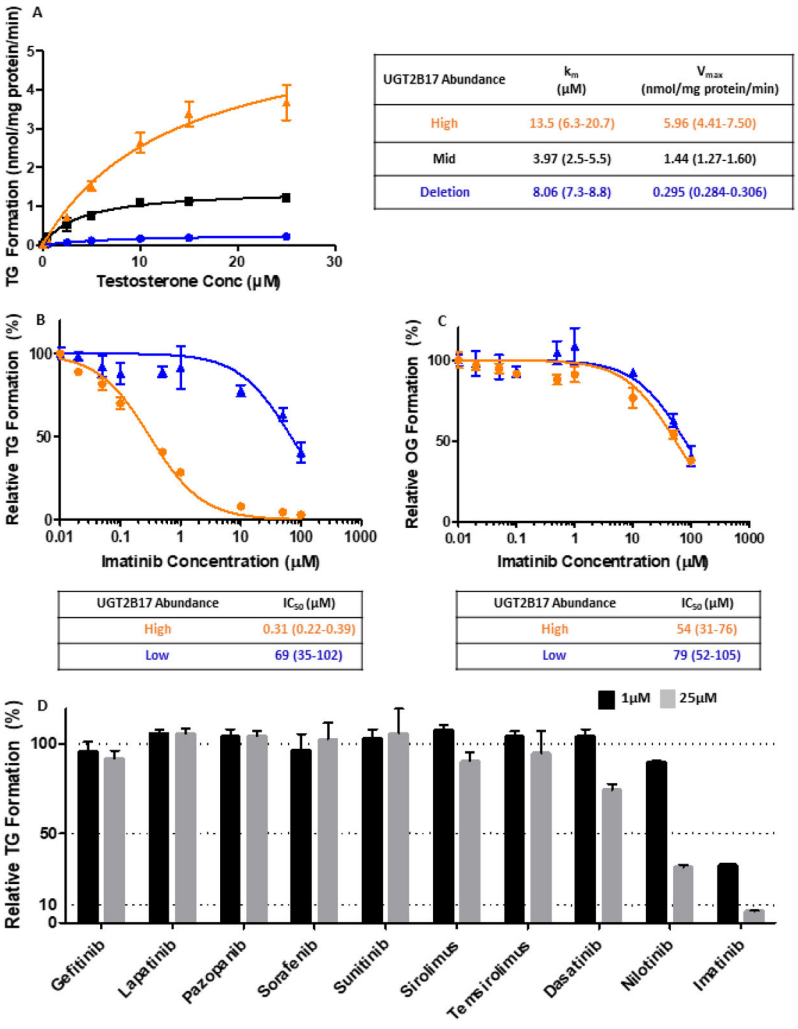

Fig. 2. Testosterone glucuronide formation kinetics and inhibition in HLMs

A. Michaelis-Menten plot of testosterone glucuronide (TG) formation in high (orange), mid (black), and null (blue) UGT2B17-expressing HLMs; **B&C.** Inhibition of imatinib in high (orange) and low (blue) UGT2B17-expressing HLMs with testosterone (B) and oxazepam (C) as probe substrates for UGT2B17 and UGT2B15, respectively; **D.** Percent TG formation in high UGT2B17-expressing HLM inhibited by various tyrosine kinase inhibitors at 1 μM and 25 μM.

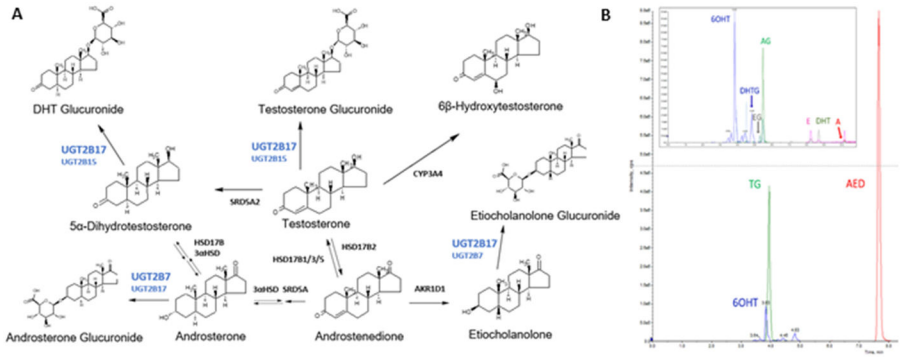

Fig. 3. Testosterone metabolism scheme

A. Simplified testosterone metabolic pathway and respective structures and enzymes; **B.** Representative LC-MS/MS chromatogram of quantified metabolites from hepatocyte.

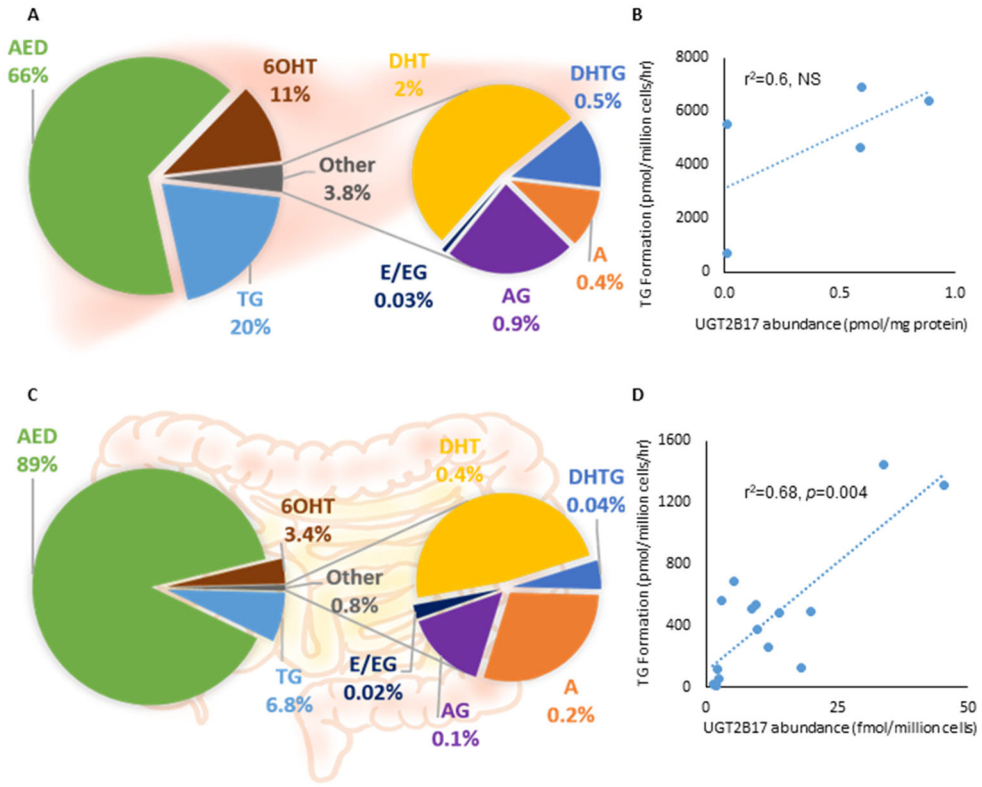

Fig. 4. Testosterone metabolism in primary human hepatocytes and enterocytes

A&C. Percent of quantified testosterone metabolites in (A) hepatocytes (n=5) and (B) enterocytes (n=16) after incubation in 50 μM testosterone for 60 and 120 minutes, respectively; **B&D.** UGT2B17 abundance vs. TG formation correlation in (B) hepatocytes (pmol/ mg membrane protein) and (D) enterocytes (fmol/ million cells). UGT2B17 quantification differed due to preexistence of BSA in enterocytes.

TG: testosterone glucuronide, DHT: dihydrotestosterone, DHTG: DHT glucuronide, A: androsterone, AG: androsterone glucuronide, AED: androstenedione, 6OHT: 6-hydroxy testosterone, E: eticholanolone, EG: eticholanolone glucuronide, NS: non-significant

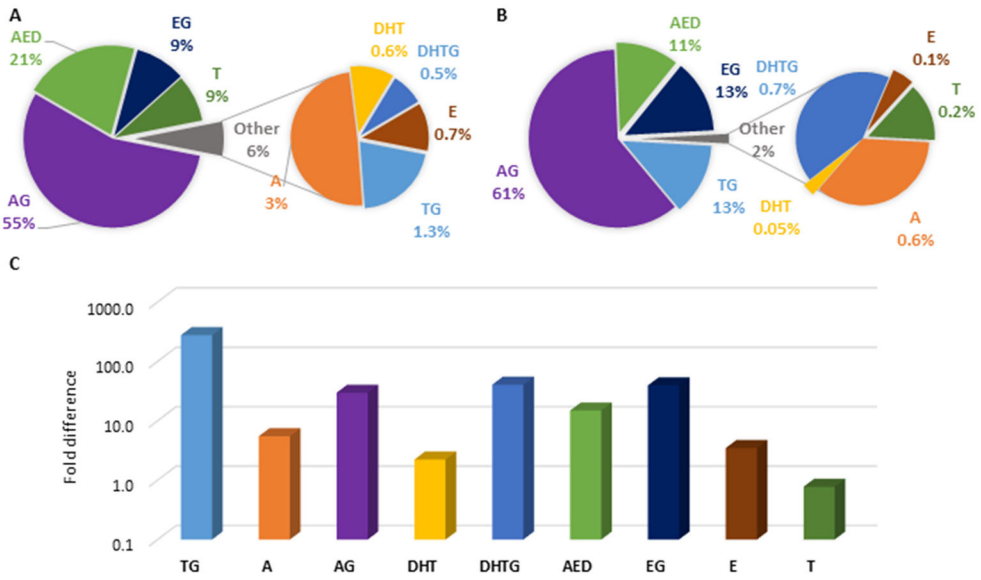

Fig. 5. Testosterone metabolism *in vivo* before and after testosterone administration. Metabolite composition in plasma

A. at baseline and **B.** after oral administration of 800 mg testosterone (T) as average of all time-points (up to 24 hours) in seven healthy adult males after chemical castration with acyline. **C.** Fold-change in absolute concentrations after 800mg T compared to baseline in log scale. Data depicted were generated from a previously published study [32].

Table 1

Sample Demographics.

	Sex	n	Age range (mean, years)	Ethnicity[a]
Human liver microsomes	Male	14	21–61 (44)	13 C, 1 A
	Female	12	45–70 (57)	12 C
Human intestinal microsomes	Male	5	22–59 (37)	5 C
	Female	1	62	
Human hepatocytes	Male	3	18–55 (33)	3 C
	Female	2	45–54 (50)	2 C
Human enterocytes	Male	8	32–60 (49)	7 C, 1 H
	Female	7	16–54 (46)	7 C
	Unknown	1	Unknown	1 Unknown

[a]Caucasian, C; Asian, A; Hispanic, H

Table 2

Optimized multiple reaction monitoring (MRM) parameters used for quantitative analysis of testosterone metabolites.

Metabolite/internal standard	Precursor ion (m/z)	Daughter Ion(s) (m/z)	DP (V)	CE (eV)	LLOQ[a] (ng/mL)
6β-Hydroxytestosterone	305.3	269.1, 121, 109	90	30, 21, 30	1 [0]; 0.5 [0]
6β-Hydroxytestosterone-d3	308.3	272.2, 290.2	80	30	
Androstenedione	287.2	109.1, 97.1	80	30	50 [0]; 50 [0]
Androsterone	291.2	255.1	60	25	10 [2]; 5 [8]
	273.1	255.1, 147	60	15, 20	
Androsterone glucuronide	449.1	255.2	70	25	5 [1]; 5 [11]
	484.3	255.2, 273.2	70	35	
Androsterone-d2	275.2	275.1, 147.1	80	5, 30	
Androsterone glucuronide-d4	453.2	259.2, 277.4	80	30, 22	
	488.3	259.3	80	30	
5α-Dihydrotestosterone	291.1	255.4, 159.1	70	22, 28	5 [0]; 1 [1]
	273.1	255.4	70	22	
5α-Dihydrotestosterone glucuronide	467.3	255.2	70	35	5 [0]; 1 [7]
	484.3	273.2	70	35	
5α-Dihydrotestosterone-d3	294.3	91, 258.2	70	69, 25	
5α-Dihydrotestosterone glucuronide-d3	470.2	294.2, 276.2, 159.2	80	30	
Etiocholanolone	273.2	255.1, 147	80	25	5 [5]; 1 [16]
	291.1	255.1	80	30	
Etiocholanolone glucuronide	484.3	273.2, 255.2	70	35	0.5 [2]; 5 [16]
	467.3	255.2	70	35	
Testosterone	289.1	109.1, 97.1	80	30	

Metabolite/internal standard	Precursor ion (m/z)	Daughter Ion(s) (m/z)	DP (V)	CE (eV)	LLOQ[a] (ng/mL)
Testosterone glucuronide	465.2	289.2, 271.2, 109.1	70	25, 30, 35	0.5 [0]; 0.5 [0]
Testosterone-d3	292.2	109.1, 97.1	80	30	
Testosterone glucuronide-d3	468.2	292.2, 274.2, 256.2	70	25, 30, 35	

[a]Lower limit of quantification (LLOQ) in hepatocytes; enterocytes. Value in brackets indicates number of samples below LLOQ, which were assigned limit of detection (LOD) as one-third of LLOQ values.

Table 3

Absolute protein abundance and inter-individual variability of UGT2B17[a] (pmol/mg microsomal protein) in human liver and intestinal microsomes (HLM and HIM).

	Mean ± SD (Range)	Fold difference[b]
HLM (n=26)	1.7 ± 2.7 (0.06–9.7)	161
HIM-Average Small Intestine (n=6)	7.6 ± 6.6 (0.06–19.2)	319
HIM-Duodenum (n=6)	6.0 ± 8.2 (0.06–22.0)	366
HIM-Jejunum (n=6)	6.8 ± 6.0 (0.06–20.8)	346
HIM-Ileum (n=6)	10.8 ± 10.8 (0.06–28.7)	479
HIM-Colon (n=6)	16.2 ± 11.4 (0.06–29.5)	492

[a] UGT2B15 abundance was 30.9±8.8 (11.8–44.7) in HLMs with 3.8-fold difference. UGT2B15 was not detected in pooled intestinal subcellular fractions and in donor-matched HIM.

[b] fold difference from LOD (0.06 pmol/mg microsomal proteins).

Table 4

Formation rate (pmol/million cells/hour) of testosterone metabolites[a] in human hepatocytes and enterocytes[b]

Cell type	Parameter	AED	TG	6OHT	DHT	DHTG	A	AG	E	EG
Hepatocytes	Mean ± SD	16154 ± 10314	4836 ± 2460	2684 ± 1527	479 ± 393	115 ± 76	95.6 ± 113	214 ± 333	<2.8[c]	<3.5[c]
	Median	13179	5515	3044	389	102	63	93	N/A	2
	Relative level (%)	66	20	11	2	0.5	0.4	0.9	0.01	0.01
	Relative to TG (fold difference)	3.3	1	0.6	0.1	0.02	0.02	0.04	0.001	0.001
Enterocytes	Mean ± SD	5743 ± 3035	437 ± 433	220 ± 128	25 ± 10	2.7 ± 4.1	15 ± 31	7.6 ± 15	<0.33[c]	<0.96[c]
	Median	5450	430	199	24	1	7	4	N/A	N/A
	Relative level (%)	89	6.8	3.4	0.4	0.04	0.2	0.1	0.01	0.04
	Relative to TG (fold difference)	13	1	0.5	0.06	0.006	0.03	0.02	0.001	0.002

[a] Androstenedione, AED; testosterone glucuronide, TG; 6-hydroxy testosterone, 6OHT; dihydrotestosterone, DHT; DHT glucuronide, DHTG; androsterone, A; A glucuronide, AG; etiocholanolone, E; E glucuronide, EG.

[b] Cryopreserved primary human hepatocyte and enterocyte suspensions were incubated in 50 μM testosterone for 60 and 120 minutes, respectively

[c] LOD = limit of detection